Multiple 0-π transitions in superconductor/insulator/ferromagnet/superconductor Josephson tunnel junctions

F. Born and M. Siegel

Institute of Micro- and Nanoelectronics Systems, Karlsruhe University, Karlsruhe, Germany

E. K. Hollmann and H. Braak

Research Center Jülich, ISG and IFF, Jülich, Germany

A. A. Golubov

Faculty of Science and Technology, University of Twente, Enschede, The Netherlands

D. Yu. Gusakova and M. Yu. Kupriyanov

Institute of Nuclear Physics, Moscow State University, Moscow, Russia

We report on experimental studies about superconducting coupling through a thin $Ni_{76}Al_{24}$ film. A patterning process has been developed, which allows in combination with the wedge shaped deposition technique the *in situ* deposition of 20 single $Nb/Al/Al_2O_3/Ni_3Al/Nb$ multilayers, each with its own well-defined Ni_3Al thickness. Every single multilayer consists of 10 different sized Josephson junctions, showing a high reproducibility and scaling with its junction area. Up to six damped oscillations of the critical current density against F-layer thickness were observed, revealing three single 0-π transitions in the ground state of Josephson junctions. Contrary to former experimental studies, the exponential decay length is one magnitude larger than the oscillation period defining decay length. The theoretical predictions based on linearized Eilenberger equations results in excellent agreement of theory and experimental results.

In the past few years there was a noticeable interest to the unconventional Josephson junctions,[1–3] in particular, to the so-called π junctions having negative critical current. These junctions provide a π shift in the ground state and were realized experimentally in SFS (superconductor-ferromagnet-superconductor) and some high-temperature superconductor structures.

The intensive experimental study of "0"-"π" transition in SFS Josephson junctions[4–13] confirms the existence of critical current oscillations upon the thickness of ferromagnetic interlayer d_f. Different structure of SFS sandwiches and superconductor/insulator/ferromagnetic/superconductor (SIFS) tunnel junctions having been fabricated up to now. They contain regions which are controlling the critical current and difficult to control in experiment and describe in theory. They are SF interfaces, dead layers, and the region in S banks with suppressed superconductivity. Contrary to that the bulk properties of F material can be better controlled and well described by theoretical models based on quasiclassical theory of superconductivity. These theories predict that for large thickness of ferromagnet the critical current of SFS junctions must exhibit a damped oscillations as a function of d_f,

$$I_c(d_f) = I_c(d_0) \frac{\left| \sin\left(\dfrac{d_f - d_1}{\xi_{F2}} \right) \right|}{\left| \sin\left(\dfrac{d_1 - d_0}{\xi_{F2}} \right) \right|} \exp\left(-\frac{d_f - d_0}{\xi_{F1}} \right). \quad (1)$$

Here d_1 is the position of the first minima, $I_c(d_0)$ is the first experimental value of $I_c(d_f)$. These two values take into ac-

count the resultant action of SF interfaces and their vicinities. The oscillations are characterized by two effective lengths. They are the decay length ξ_1, and the length ξ_2, which determines the period of oscillations. In dirty limit the expressions for $\xi_{1,2}$ follow from the Usadel equations[14] and have the form

$$\xi_{1,2} = \sqrt{\frac{D_f}{\sqrt{(\pi T)^2 + E_{ex}^2} \pm \pi T}}, \quad (2)$$

where D_f and E_{ex} are the diffusive coefficient and exchange field of ferromagnetic material, respectively. In the clean limit one can easily get from Eilenberger equations that[15]

$$\xi_1^{-1} = \xi_0^{-1} + \ell^{-1}, \quad \xi_0 = \frac{v_F}{2\pi T}, \quad \xi_2 = \xi_H = \frac{v_F}{2E_{ex}}, \quad (3)$$

where $l \gg \xi_0$ is the electron mean free path and v_F is the Fermi velocity in a ferromagnet.

It is clearly seen from Eqs. (2) and (3) that for dirty materials $\xi_2 > \xi_1$, and in the limit of large exchange energy, $E_{ex} \gg \pi T$, the characteristic lengths are nearly equal $\xi_1 \simeq \xi_2$. In the clean limit these ξ_1 and ξ_2 are completely independent.

Our analysis of both the bulk properties of ferromagnet materials[16] and the experimental data[4–13] has shown (see Table I) that in dilute ferromagnets[5,8,10,11] the electron mean free path is very small providing the fulfilment of the dirty limit conditions for the F interlayer. In these experiments $\xi_1 \simeq \xi_2$ as it follows from Eq. (2). Contrary to that, in the structures with Ni interlayer the relation between ξ_2 and ξ_1 is just the opposite so that a more complex model[17] should be used for the data interpretation. It is necessary to point out

TABLE I. Characteristic lengths in ferromagnetic materials for SFS Josephson junctions.

Reference	ξ_1 (nm)	ξ_2 (nm)	F material	v_F (m/s)	E_{ex} (K)
8	1.2	1.6	$Fe_{20}Ni_{80}$	2.2×10^5	1100
11	1.8	2	$Pd_{0.9}Ni_{0.1}$	2×10^5	400
10	1.2	3.5	$Cu_{0.53}Ni_{0.47}$		850
5			$Cu_{0.52}Ni_{0.48}$		
9	1.7	1	Ni	2.8×10^5	2300
This work	4.6	0.45	Ni_3Al	1.5×10^5	1000

that in all previous experiments (except Ref. 13) the structures were not fabricated in one run, so that the certain degree of nonreproducibility of magnetic constants of F materials occurred for junctions with different d_f. This results in increase of spread of data with increasing d_f and did not permit to observe the large amount of oscillations.

In this work, we improved the reproducibility of the junction parameters by preparing the structures in one run with F-layer thickness between 10 nm and 20 nm. We succeeded in observation of up to six damped oscillations of critical current with F-layer thickness. To do this we have used the "wedge" shaped F-layer technique and a new ferromagnetic material (Ni_3Al). We experimentally obtained a one order of magnitude difference between ξ_1 and ξ_2 which is consistent with theory based on the Eilenberger equations.[15]

The bottom electrode of SIFS samples consists of Nb/Al/Nb/Al and was deposited on oxidized 2 inch Si wafers with argon magnetron sputtering. The top 10 nm thick Al layer has been oxidized for 2 minutes in a 0.1 mbar pure oxygen. The following Ni_3Al interlayer was sputtered with neon gas from one single target. The target composition of the alloy was determined by Rutherford backscattering (RBS) and is $Ni_{74}Al_{26}$. A 30 nm Nb top layer was deposited *in situ* to prevent the interlayer from oxidation. A schematic cross section of the deposited multilayer is shown in the inset of Fig. 1. To achieve a thickness gradient of the Ni_3Al layer the position of the target above the substrate has been shifted during deposition for several centimeter. This permits us to produce a rather linear thickness gradient over the whole 2 inch substrate (see Fig. 1).

The transport measurements were performed at 4.2 K. Figure 2 shows the dependence of the critical current, I_C, upon external magnetic field H. The rather optimal agreement between experimental results and the Fraunhofer function fit indicates a uniform and homogenous current distribution in the junction. The current-voltage characteristics (CVC) of several Josephson junctions can be seen in Fig. 3. They show a clear superconducting tunnelling behavior with a hysteresis in its curves. These four curves belong to one defined Ni_3Al layer thickness of 12.5 nm. The current is normalized to the current density, since the four junctions differ in their sizes. It can be seen in Fig. 3, that the current density differs only several percent, thus showing a good reproducibility of our junctions. This result also indicates that within one patterned line the F-layer thickness variation could be neglected. The thickness gradient has been characterized and proofed with RBS measurements. The variations are several
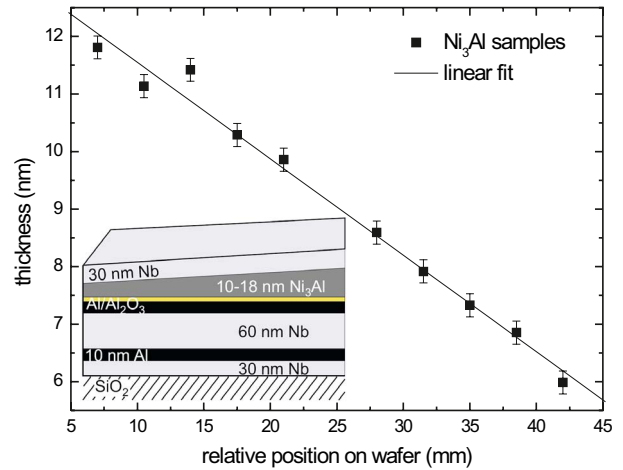

FIG. 1. (Color online) $Ni_{76}Al_{24}$ film thickness measured at different positions on a 2 inch Si wafer with the RBS method. Inset, layer sequence in a cross section.

Ångstroms. We developed a patterning process that allows the creation of 20 different separated 500 μm wide lines, distributed homogeneous along the F-layer thickness gradient over the 2 inch wafer. Each lines consists of 10 different sized circular Josephson junctions. The junction area differs from 5 to 1000 μm^2. The variation of F-layer thickness inside an individual junction is negligible small. The ferromagnetic properties of Ni_3Al films depend on neon pressure. Details will be presented elsewhere.[18] The magnetic properties of the Ni_3Al layers were measured with a SQUID magnetometer. The Curie temperature for a 250 nm thick Ni_3Al layer is 74 K.

The Ni_3Al thickness dependence of the critical current density can be seen in Fig. 4. Several Josephson junctions of each line were measured and plotted versus their corresponding Ni_3Al-layer thickness. A clear oscillating behavior of the critical current density of more than 60 single junctions ver-
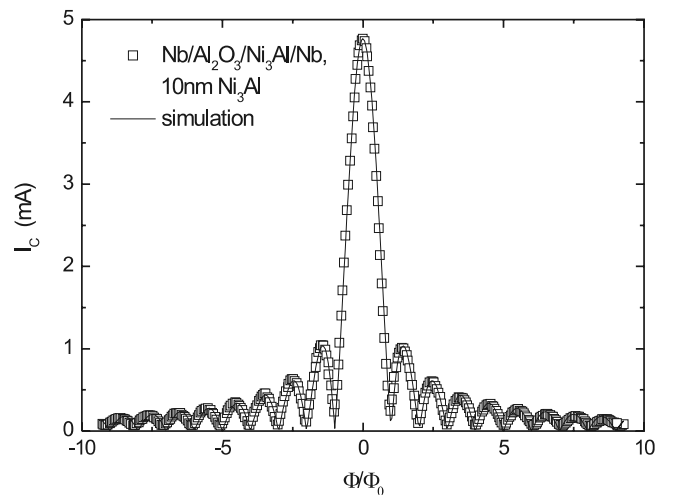

FIG. 2. Fraunhofer pattern of a typical circular Nb/Al/Al_2O_3/Ni_3Al/Nb Josephson junction, measured at 4.2 K (rectangles). The junction size is about 1000 μm^2. The solid line results from a fit to the Fraunhofer function.
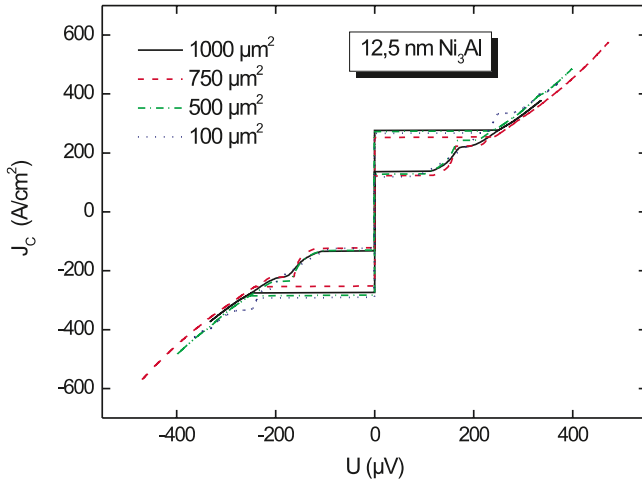
FIG. 3. (Color online) Current density vs voltage characteristics of four different Josephson junctions from one patterned line with different junction sizes, measured at 4.2 K. The size of junctions changes from 100 μm^2 to 1000 μm^2. The F-layer thickness is 12.5 nm.

sus d_F is shown, indicating three different 0-π transitions. The amplitude of oscillations decays exponentially with a characteristic decay length of $\xi_1 = 4.6$ nm. It should be pointed out that the corresponding oscillation period, given by $\pi\xi_2$, is one magnitude smaller, namely $\xi_2 = 0.45$ nm. There is a rather good agreement of the theoretical fit after Eq. (1) with these two decay length's, see the solid line in Fig. 4. A magnetically dead layer has been observed by measuring the dependence of magnetization on Ni$_3$Al-layer thickness. Details will be presented elsewhere.[18] We determined a thickness of the dead layer around 5 nm to 8 nm for SF and FS interfaces. Figure 4 shows that 0-π transitions disappear for a Ni$_3$Al-layer thickness below 10 nm. We explain this finding with the existence of a magnetically dead layer at SF and FS interfaces. To find a theoretical explana-
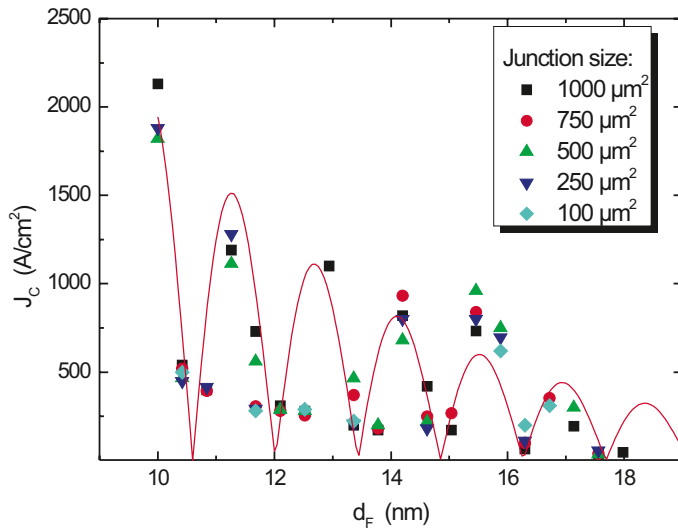

FIG. 4. (Color online) Critical current density of up to 60 single SIFS Josephson junctions against the F-layer thickness. The solid line indicates a theoretical fit after Eq. (1) with the two fitting parameters $\xi_1 = 4.6$ nm and $\xi_2 = 0.45$ nm.

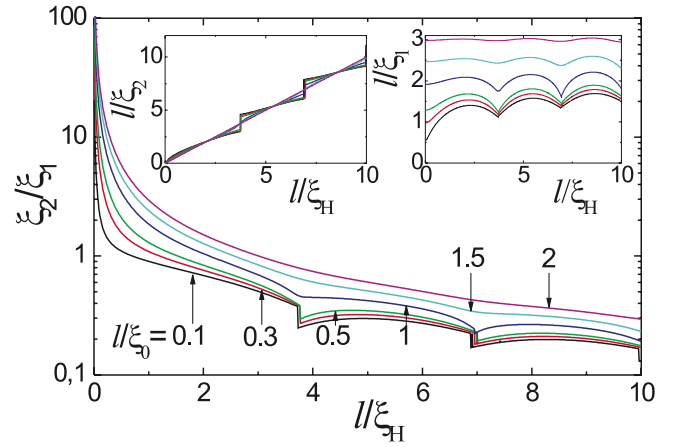

FIG. 5. (Color online) Dependence of the ratio ξ_2/ξ_1 on inverse magnetic length l/ξ_H calculated for different ratios of l/ξ_0. Left-hand inset: Inverse decay length l/ξ_2 vs inverse magnetic length l/ξ_H for different ratios of l/ξ_0. Right-hand inset: Inverse decay length l/ξ_1 vs inverse magnetic length l/ξ_H for different ratios of l/ξ_0.

tion for the large difference between ξ_1 and ξ_2 we start with linearized Eilenberger equations which are valid at the distances from SF interface larger than ξ_1,

$$2f + \frac{v_f \cos\theta}{\omega + iE_{ex}}\frac{d}{dx}f = \frac{\langle f\rangle - f}{\tau(\omega + iE_{ex})}, \quad \langle(\ )\rangle = \int_0^\pi (\ )\sin\theta\, d\theta. \tag{4}$$

Here θ is the angle between direction of the Fermi velocity and interface normal, $\tau = v_F/l$ is the scattering time.

The solution of this equation has the form[19]

$$f(x,\theta) = C(\theta)\exp\left(-\frac{x}{\xi_{eff}}\right), \quad \xi_{eff}^{-1} = \xi_1^{-1} + i\xi_2^{-1}, \tag{5}$$

where ξ_{eff} is the effective decay length which is independent on θ and $C(\theta)$ is an integration constant. Substitution of Eq. (5) into Eq. (4) gives

$$C(\theta) = \frac{\eta\langle C\rangle}{1 - k^2\cos^2\theta}, \quad \eta = \frac{\ell^{-1}}{\xi_0^{-1} + \ell^{-1} + i\xi_H^{-1}}, \quad k = \frac{\eta\ell}{\xi_{eff}}. \tag{6}$$

Integration of Eq. (6) over angle θ provides the equation for ξ_{eff},

$$\tanh\frac{\ell}{\xi_{eff}} = \frac{\xi_{eff}^{-1}}{\xi_0^{-1} + \ell^{-1} + i\xi_H^{-1}}. \tag{7}$$

In the dirty limit, $\ell \ll \xi_0\xi_H(\xi_H + \sqrt{\xi_0^2 + \xi_H^2})^{-1}$ and in the clean limit $1 + \ell\xi_0^{-1} \gg \frac{1}{2}\max\{\ln(1 + \ell\xi_0^{-1}), \ln(\ell\xi_H^{-1})\}$, the solution of Eq. (7) reduces to Eqs. (2) and (3), respectively. The results of numerical solution of Eq. (7) are presented in Fig. 5.

There are steps on $\xi_2^{-1}(\xi_H^{-1})$ and ξ_2/ξ_1 vs ξ_H^{-1} dependencies (see Fig. 5) accompanied by the minima on $\xi_1^{-1}(\xi_H^{-1})$ curves (see Fig. 5, right-hand inset). The ratio of ξ_2/ξ_1 falls very rapidly with increase of ξ_H. It follows from Fig. 5 that the experimental value of this ratio $\xi_2/\xi_1 \approx 0.1$ can be achieved

at $l \approx 10\xi_H$. For the estimated earlier parameters $\xi_1 \approx 4.5$ nm and $\xi_2 \approx 0.5$ nm from Fig. 5, left-hand inset and Fig. 5, right-hand side inset we get nearly equal values for the electron mean free path $l \approx 1.4\xi_1 \approx 6.3$ nm and $l \approx 11\xi_2 \approx 5$ nm, respectively. In the last estimation it was also supposed that $l/\xi_0 \approx 0.1$, resulting in $\xi_0 \approx 50$ nm and Fermi velocity $v_F = 1.8 \times 10^5$ m/s. With this value of v_F and $\xi_H \approx 0.1 l \approx 0.5$ nm we arrived at $E_{ex} \approx 1300$ K ≈ 0.11 eV. This combination of parameters is not unique. Starting from $l \approx 20\xi_H$ and $l/\xi_0 \approx 0.3$ one can get $l \approx 9.5$ nm, $\xi_0 \approx 30$ nm, $v_F = 1.2 \times 10^5$ m/s, and $E_{ex} \approx 900$ K ≈ 0.08 eV. These parameters are consistent with the previous experimental data integrated into Table I.

The discovered behavior of ξ_2 and ξ_1 is quite general and must be also observed in structures without ferromagnetic ordering. An example is a normal filament of finite length, which is placed between superconducting banks and is biased by a dc supercurrent. It was shown,[20] that the minigap induced to this filament from the S electrodes is not a monotonous function of phase difference across the structure. This behavior could be also explained in terms of specific dependencies of ξ_2 and ξ_1 upon electron mean free path in current biased systems.

Summarizing the presented results we conclude that utilization of the new ferromagnetic material, Ni_3Al, as well as the wedge technique for its deposition permits the experimental demonstration as much as six oscillations of the critical current as a function of thickness of ferromagnetic layer. High reproducibility of the junctions parameters, their scaling with the area, suppression of oscillation observed after only one change in operation-routing sequence, namely, replacement of Ar by Ne during the sputtering of Ni_3Al, clearly manifests that observed effect is due to magnetic ordering in Ni_3Al film. The fact of this ordering has been also confirmed by independent examination of magnetization of the Ni_3Al films. It is important also to mention that Ni_3Al is an intermetallide. This metal is widely used and has been well studied before.[16] It successfully combines the relatively small values of exchange integral with the transport properties close to that of strong pure ferromagnets. We believe that it will substitute the dilute ferromagnetic alloys in the SFS Josephson junction technology. The experimental results are consistent with the theoretical predictions made in the frame of the Eilenberger equations. Moreover, it was demonstrated that the intuitive knowledge about the relation between ξ_2 and ξ, which is based on the dirty theories, has a very limited field of applications and cannot be used for $\xi_H > 5l$ or for $E_{ex}\tau > 0.1$. In particular, we found that the increase of E_{ex} is not always accompanied by the decrease of ξ_1 and there is some range of parameters when ξ_1 even may increase with E_{ex}. The fact that one may combine reasonably large decay length with the smaller period of oscillations looks rather attractive for possible applications of SFS Josephson junctions.

---

[1] A. A. Golubov, M. Y. Kupriyanov, and E. Il'ichev, Rev. Mod. Phys. **76**, 411 (2004).

[2] A. I. Buzdin, Rev. Mod. Phys. **77**, 935 (2005).

[3] F. S. Bergeret, A. F. Volkov, and K. B. Efetov, Rev. Mod. Phys. **77**, 935 (2005).

[4] V. V. Ryazanov, V. A. Oboznov, A. Y. Rusanov, A. V. Veretemikov, A. A. Golubov, and J. Aarts, Phys. Rev. Lett. **86**, 2427 (2001).

[5] H. Sellier, C. Baraduc, F. Lefloch, and R. Calemczuk, Phys. Rev. B **68**, 054531 (2003).

[6] Y. Blum, A. Tsukernik, M. Karpovski, and A. Palevski, Phys. Rev. B **70**, 214501 (2004).

[7] C. Surgers, T. Hoss, C. Schonenberger, and C. Strunk, J. Magn. Magn. Mater. **240**, 598 (2002).

[8] C. Bell, R. Loloee, G. Burnell, and M. G. Blamire, Phys. Rev. B **71**, 180501(R) (2005).

[9] V. Shelukhin, A. Tsukernik, M. Karpovski, Y. Blum, K. B. Efetov, A. Volkov, T. Champel, M. Eschrig, T. Lofwander, G. Schon, and A. Palevski, Phys. Rev. B **73**, 174506 (2006).

[10] V. A. Oboznov, V. V. Bol'ginov, A. K. Feofanov, V. V. Ryazanov, and A. I. Buzdin, cond-mat/0508573 (to be published).

[11] T. Kontos, M. Aprili, J. Lesueur, F. Genet, B. Stephanidis, and R. Boursier, Phys. Rev. Lett. **89**, 137007 (2002).

[12] M. Weides, K. Tillmann, and H. Kohlstedt, Physica C **437-438**, 349 (2006).

[13] H. Sellier, C. Baraduc, F. Lefloch, and R. Calemczuk, Phys. Rev. Lett. **92**, 257005 (2004).

[14] A. I. Buzdin, B. Bujicic, and M. Y. Kupriyanov, Sov. Phys. JETP **74**, 124 (1992).

[15] G. Eilenberger, Z. Phys. **214**, 196 (1968).

[16] M. Y. Kupriyanov, A. A. Golubov, and M. Siegel, Proc. SPIE (to be published).

[17] F. S. Bergeret, A. F. Volkov, and K. B. Efetov, Phys. Rev. B **64**, 134506 (2001).

[18] F. Born, M. Siegel, E. Hollmann, H. Braak, M. Y. Kuprianov, and V. Volpyas (unpublished).

[19] M. Y. Kupriyanov, Sov. J. Low Temp. Phys. **7**, 342 (1981).

[20] M. V. Kalenkov, H. Kloos, and A. D. Zaikin (private communication).